Front. Optoelectron. China 2011, 4(1): 114–120
DOI 10.1007/s12200-011-0152-y

RESEARCH ARTICLE

Surface-enhanced fluorescence from copper nanoparticles on silicon nanowires

Shujuan ZHUO[1], Mingwang SHAO (✉)[1], Liang CHENG[1], Ronghui QUE[1], Dorthy Duo Duo MA[2], Shuit Tong LEE (✉)[2]

1 Institute of Functional Nano & Soft Materials (FUNSOM), Jiangsu Key Laboratory for Carbon-Based Functional Materials & Devices, Soochow University, Suzhou 215123, China
2 Center of Super-Diamond and Advanced Films and Department of Physics and Materials Science, City University of Hong Kong, Hong Kong, China

Abstract A method to enhance surface plasmon coupled fluorescence from copper nanoparticles on silicon nanowires is presented. Owing to resonant plasmons oscillation on the surface of Cu/Si nanostructure, the fluorescence peaks of several lanthanide ions (praseodymium ions, Pr^{3+}, neodymium ions Nd^{3+}, holmium ions Ho^{3+}, and erbium ions Er^{3+}) were markedly enhanced with the enhancement of maximal 2 orders of magnitude, which was larger than that caused by unsupported Cu nanoparticles. These results might be explained by the local field overlap originated from the closed and fixed copper nanoparticles on silicon nanowires.

Keywords Cu/Si nanostructure, surface-enhanced fluorescence, lanthanide ions, resonant plasmons oscillation

1 Introduction

Surface-enhanced fluorescence (SEF) is known for more than a few decades [1]. A metallic particle near a fluorophore can influence both its excitation and emission, eventually leading to significantly enhanced spectral properties [2–5]. The enhancement is suggested to occur via a coupling interaction of the fluorophore and the electric field around the metal particle, which can be induced by incident light or by the excited fluorophore [6–10]. This effect can bring an increase in the quantum yield and improve the efficiency of light absorption [11–13].

Recently, research on the enhanced fluorescence properties of lanthanide ions such as Pr^{3+} and Nd^{3+} [14–17] in low dimensional semiconductors has attracted much interest because of their potential application in optoelectronic devices.

The photoluminescence (PL) properties of lanthanide ions have been investigated for decades [18–20]. An attractive feature of luminescent lanthanide ions is their line-like emission, which results in a high color purity of the emitted light. Actually lanthanide ions have been considered the most important optical activators for luminescent devices.

Emission of light from lanthanide ions is a fundamentally important process with a continuously expanding range of applications in contemporary electronic devices. However, the photon absorption cross section of some trivalent Ln^{3+} ions (Pr^{3+}, Nd^{3+}, etc) is very small due to the dipole-forbidden nature of the intra^{-4}f transitions and, thus, the intensity of the PL is relatively low. In order to overcome the small absorption cross section, coupling Ln^{3+} ions with metal nanoparticles was a valuable strategy.

Metal nanoparticles were ready to agglomerate during their application [21]. To overcome the limitation, in the paper, the Cu/Si nanomaterials were employed in investigating the SEF process of Ln^{3+} (Ln = Pr, Nd, Ho, and Er). It showed that the emission of intrinsically fluorescent Ln^{3+} could be significantly enhanced by Cu/Si nanostructure, which had a greater enhancement than the unsupported Cu nanoparticles. Furthermore the preliminary explanation of excellent SEF based on Cu/Si nanostructure was proposed.

2 Experiment

2.1 Materials

Pr_6O_{11}, Nd_2O_3, Ho_2O_3, Er_2O_3 and $CuSO_4 \cdot 5H_2O$ were

Received October 18, 2010; accepted December 30, 2010

E-mail: mwshao@suda.edu.cn, apannale@cityu.edu.hk

purchased from Alfa Aesar Co. Pr_6O_{11}, Nd_2O_3, Ho_2O_3 and Er_2O_3 powders were dissolved in concentrated nitric acid to make a 0.1 M stock solution. $CuSO_4$ was prepared to 5.0×10^{-3} M with doubly distilled water.

Other reagents were of analytical grade without further purification. Doubly distilled water was used throughout.

2.2 Synthesis of silicon nanowires (SiNWs) and modification with Cu nanoparticles

The SiNWs were prepared via a simple thermal evaporation of SiO powder using the oxide-assisted growth method developed by us [22]. The as-synthesized SiNWs (0.008 g) were etched with 5 mL 5% HF aqueous solution for 1 min to get rid of their outer oxide layer, rinsed with distilled water, and then immersed in 15 mL 1×10^{-3} M $CuSO_4$ aqueous solution. Then the yellow SiNWs gradually turned black, which indicated that they were modified with Cu nanoparticles. The total amount of copper on the surface was determined to be 75 μg. Then the Cu/Si nanomaterials were dispersed in 2 mL distilled water under the violent ultrasonic irradiation.

2.3 Synthesis of unsupported Cu nanoparticles

Unsupported Cu nanoparticles were prepared by reducing $CuSO_4$ solution directly to Cu nanoparticles with the method reported before [23].

2.4 Characterization

The as-prepared products were characterized by X-ray diffraction (XRD), which was carried out on a Philips X'pert PRO MPD diffractometer with Cu Kα radiation (λ = 0.15406 nm). A scanning rate of $0.05°\cdot s^{-1}$ was applied to record the pattern in the 2θ range of 25°–80°. The morphology of the SiNWs was characterized by scanning electron microscopy (SEM, FEI Co., model Quanta-200) with an energy dispersive X-ray (EDS) spectrum. Fluorescence spectra were measured with a Fluoromax-4 spectrofluorimeter.

3 Results and discussion

3.1 Synthesis and modification of SiNWs

The SEM image in Fig. 1 reveals that the sample takes the shape of a wire, which is smooth and uniform with length up to several micrometers. The elemental analysis of SiNWs shows no peaks of other elements except Si and O, indicating a high purity of the products.

Figure 2(a) shows the XRD pattern of the as-prepared SiNWs, and all diffraction peaks can be indexed as the cubic phase of Si. The cell parameter is calculated to be a = 0.5435±0.0054 nm, which is in agreement with the value

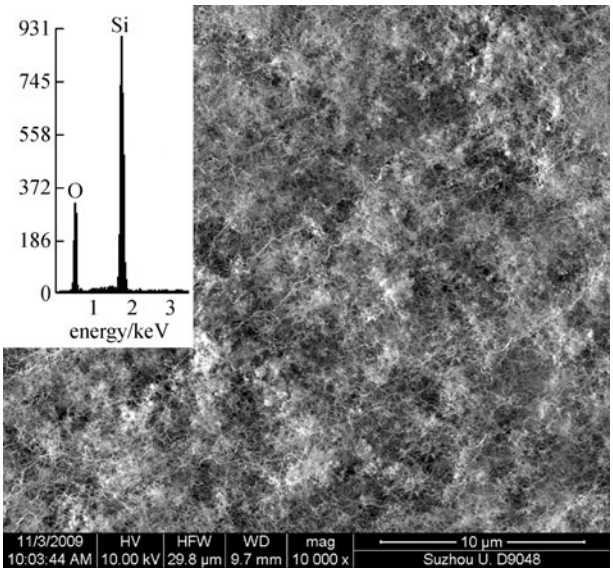

Fig. 1 SEM image and EDS (insert) of SiNWs

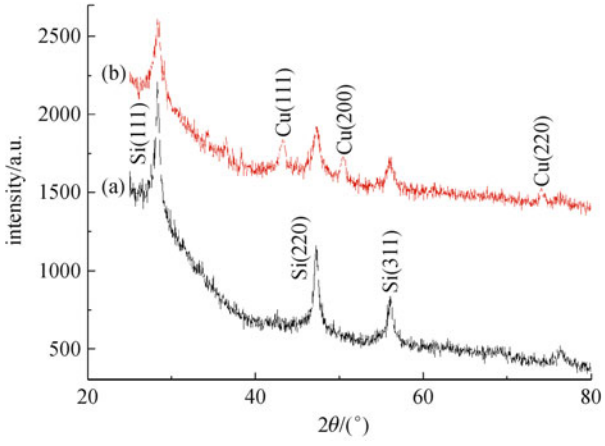

Fig. 2 XRD patterns of (a) SiNWs; (b) Cu/Si nanostructure

of face-centered cubic silicon a = 0.5430 nm (Joint Committee of Powder Diffraction Standards, JCPDS card No. 27-1402). The XRD pattern of SiNW-supported Cu nanoparticles is shown in Fig. 2(b). No other characteristic peaks are observed except Cu and Si. The XRD pattern demonstrates that the SiNWs have been modified with Cu nanoparticles. The calculated cell parameter of Cu is a = 0.3616±0.0003 nm, which is in agreement with the reported value, a = 0.3615 nm (JCPDS card No. 04-0836).

3.2 Enhancement fluorescence experiment of Cu/Si nanostructure

In Fig. 3, the Ln^{3+} (Ln = Pr, Nd, Ho, and Er) displayed weak fluorescence emission at the peaks of 595 nm, 604 nm, 640 nm of Pr^{3+}, 592 nm of Nd^{3+} upon excitation at 470, and 550 nm of Ho^{3+}, 533 nm of Er^{3+} upon

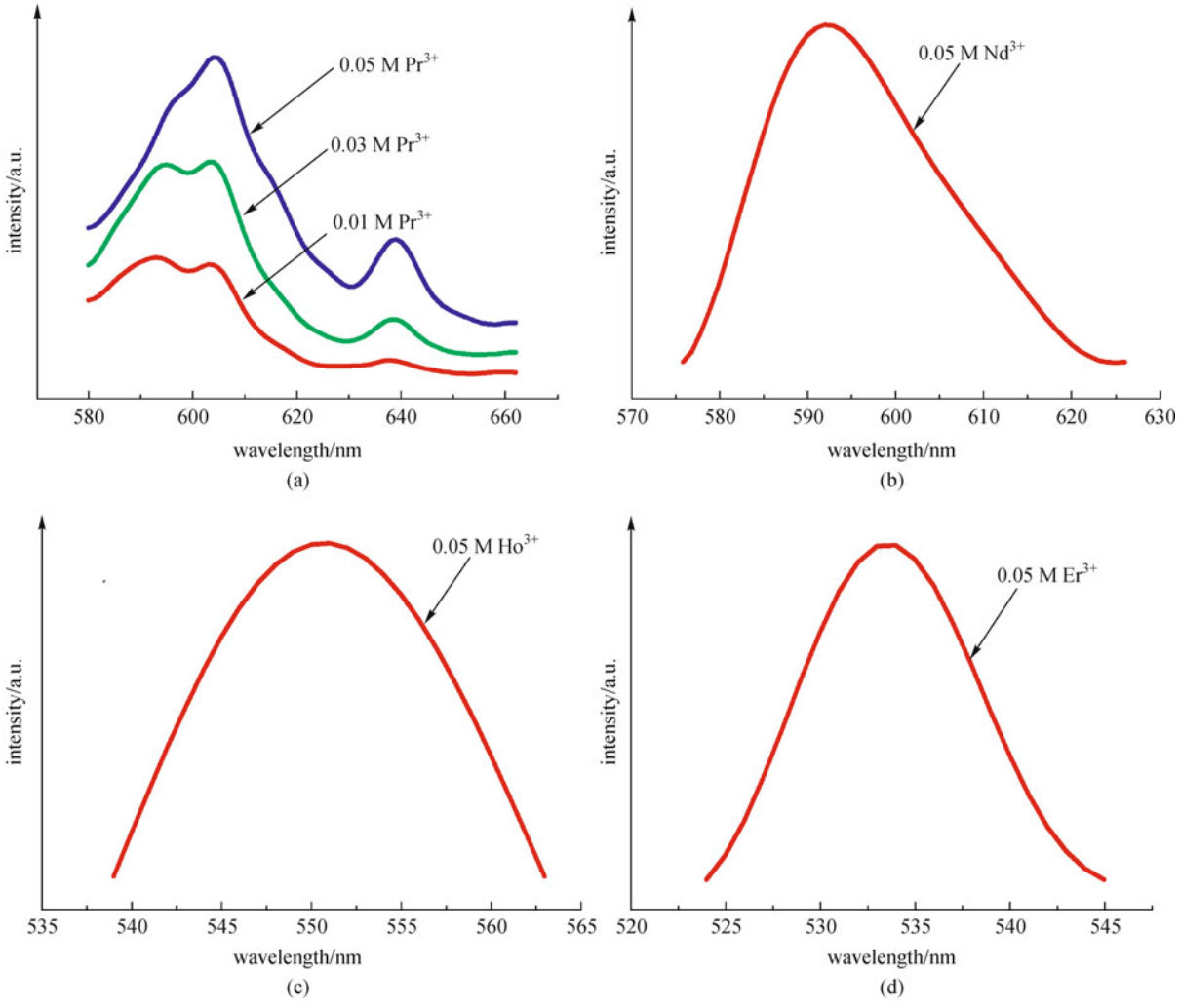

Fig. 3 Fluorescence spectra of Ln^{3+} free of Cu/Si nanomaterials. (a) Different concentrations of Pr^{3+}; (b) 0.05 M Nd^{3+}; (c) 0.05 M Ho^{3+}; (d) 0.05 M Er^{3+}

excitation at 430 nm, which were attributed to be the 4*f* inter-level $^1I_6 \rightarrow {}^3F_3$ (595 nm), $^1D_2 \rightarrow {}^3H_4$ (604 nm) and $^3P_0 \rightarrow {}^3F_2$ (640 nm) of Pr^{3+}, $^2F_{7/2} \rightarrow {}^2P_{1/2}$ (592 nm) of Nd^{3+}, $^5G_2 \rightarrow {}^5I_5$ (550 nm) of Ho^{3+} and $^4S_{3/2} \rightarrow {}^4I1_{5/2}$ (533 nm) transitions of Er^{3+}.

Figures 4(a), (c), and (e), show the fluorescence spectra of Pr^{3+} at the different concentrations with the increment of Cu/Si amount (50 μL each time). As can be seen, the fluorescence intensity increases gradually with the addition of Cu/Si nanomaterials. After that, the intensity keeps steady with further growth of the Cu/Si. In addition, the enhancement decreased (from 167-fold to 12-fold at 640 nm and 30-fold to 9-fold at 604 nm) when Pr^{3+} concentration changed from 0.01 to 0.05 M. Moreover, the peak at 604 nm dominated gradually and finally resulted in the mergence of the peak about 595 nm.

To make a comparison, unsupported Cu nanoparticles were used. It can be observed from Figs. 4(b), (d), and (f) that the fluorescence intensity of Pr^{3+} was also enhanced with the addition of the unsupported Cu nanoparticles. The enhancement was about 59-fold to 8-fold at 640 nm and 9-fold to 6-fold at 604 nm, respectively. The fluorescence emission increased to the maximum and then keeps steady, which was in agreement with the Cu/Si nanostructure. However, the enhancement factor was smaller than that caused by Cu/Si nanostructure.

Figures 5(a), 6(a), and 7(a) show the fluorescence spectra of other Ln^{3+} at the concentration of 0.05 M (Ln = Nd, Ho, and Er) in the presence of Cu/Si nanomaterials. An enhancement factor of 127-fold for Nd^{3+}, 59-fold for Ho^{3+} and 52-fold for Er^{3+} could be obtained. However, in Figs. 5(b), 6(b) and 7(b), the enhancement was only about 45-fold, 25-fold and 21-fold for Nd^{3+}, Ho^{3+} and Er^{3+} respectively when unsupported Cu nanoparticles were employed.

The above results indicated that the enhancement of Cu/Si nanostructure is better than that of the unsupported Cu nanoparticles, which drew our interest.

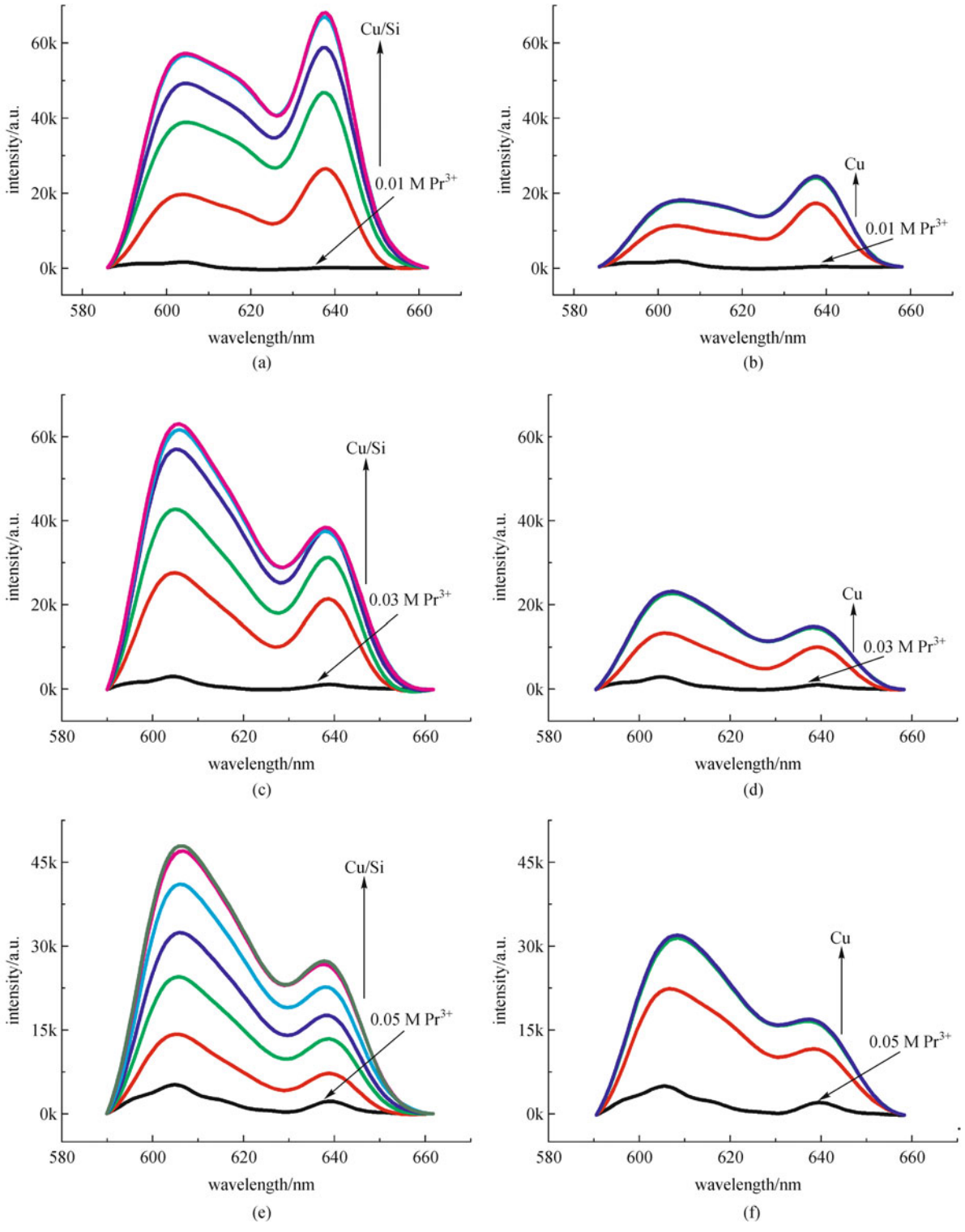

Fig. 4 Fluorescence spectra of different Pr^{3+} concentrations as adding of (a), (c), (e) Cu/Si nanomaterials, and (b), (d), (f) unsupported Cu nanoparticles

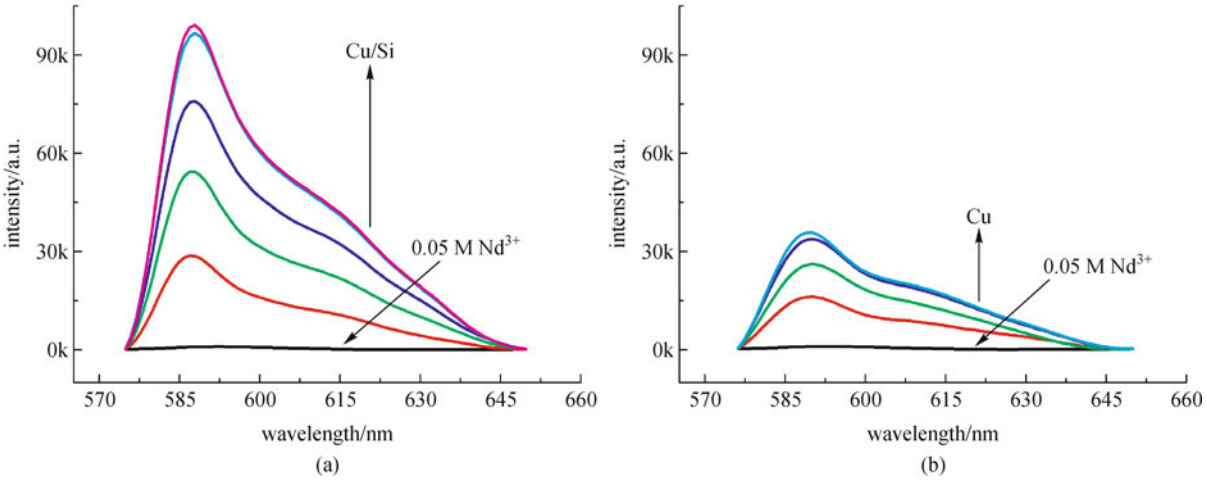

Fig. 5 Fluorescence spectra of Nd^{3+} as adding of different nanoparticles. (a) Cu/Si nanomaterials; (b) unsupported Cu nanoparticles

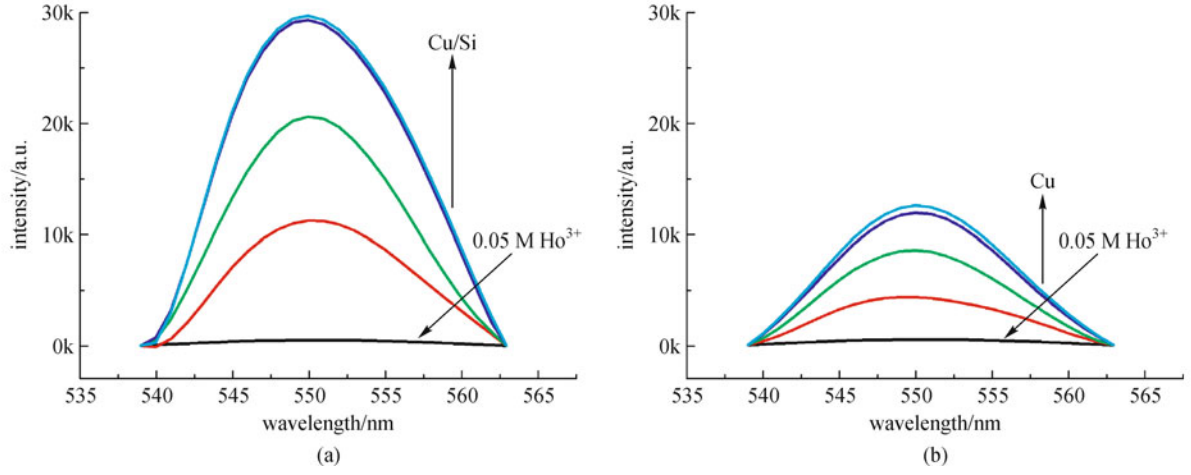

Fig. 6 Fluorescence spectra of the Ho^{3+} as adding of different nanoparticles. (a) Cu/Si nanomaterials; (b) unsupported Cu nanoparticles

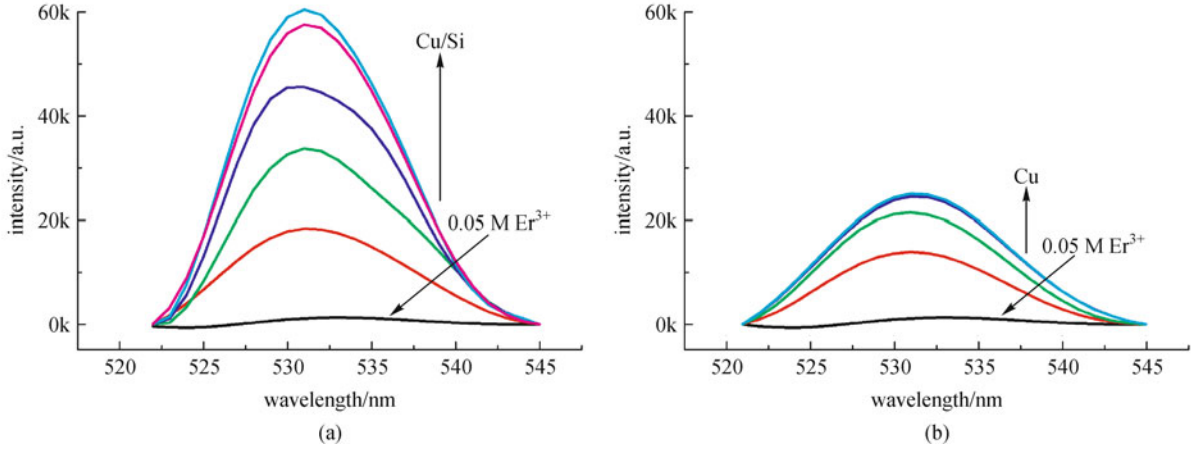

Fig. 7 Fluorescence spectra of Er^{3+} as adding of different nanoparticles. (a) Cu/Si nanomaterials; (b) unsupported Cu nanoparticles

One explanation might result from the overlap of enhanced local fields. The essential difference between these nanomaterials is that Cu/Si nanostructure has silicon carrier, The excellent SEF feature of Cu/Si nanostructure might be attributed to the unique fearures of H-SiNWs (SiNWs after HF-treatment) in anchoring metal NPs (e.g., Au, Ag, Pd, Cu) firmly and in a dispersed fashion on SiNWs surfaces [24,25]. The Cu/Si nanostructure is kept from congregating and growing larger because the small Cu nanoparticles are fixed by the SiNWs and the interparticle overlap might lead to larger field enhancement factors [26].

The unsupported Cu nanoparticles also have SEF feature. However, they are apt to agglomerate and may gradually grow large during the SEF process. Large particles might meet stronger steric hindrances in the couplings, whereas Cu nanoparticles immobilized on the SiNWs are kept from growing large; and the distances among the particles were close enough to favor the enhanced fields' overlapping, which caused great SEF effect.

4 Conclusions

In conclusion, the Cu/Si nanostructure was prepared using SiNWs as a carrier, which has the advantage of easy surface modification with various metals. The as-fabricated Cu/Si nanostructure was comparatively stable and was able to prevent Cu nanoparticles from aggregating, and thus enhanced the fluorescence of Ln^{3+} dramatically. The enhancement of Cu/Si nanomaterials are larger than that on unsupported Cu nanoparticles. This result might be attributed to the large local plasmons oscillation resulted from the interparticle overlap on the SiNWs. This easy fabrication of Cu/Si nanostructure with excellent properties enables itself to find wider applications.

Acknowledgements The work was supported by the National Basic Research Program of China (No. 2006CB933000).

References

1. Chance R R, Prock A, Silbey R. Molecular fluorescence and energy transfer near interfaces. Advances in Chemical Physics, 1978, 37: 1–65
2. Ray K, Badugu R, Lakowicz J R. Metal-enhanced fluorescence from CdTe nanocrystals: a single-molecule fluorescence study. Journal of the American Chemical Society, 2006, 128(28): 8998–8999
3. Lakowicz J R. Plasmonics in biology and plasmon-controlled fluorescence. Plasmonics, 2006, 1(1): 5–33
4. Aslan K, Holley P, Geddes C D. Metal-enhanced fluorescence from silver nanoparticle-deposited polycarbonate substrates. Journal of Materials Chemistry, 2006, 16(27): 2846–28525.
5. Ray K, Chowdhury M H, Lakowicz J R. Aluminum nanostructured films as substrates for enhanced fluorescence in the ultraviolet-blue spectral region. Analytical Chemistry, 2007, 79(17): 6480–6487
6. Mertens H, Koenderink A F, Polman A. Plasmon-enhanced luminescence near noble-metal nanospheres: Comparison of exact theory and an improved Gersten and Nitzan model. Physical Review B: Condensed Matter and Materials Physics, 2007, 76(11): 115123-1–115123-12
7. Lakowicz J R. Radiative decay engineering: biophysical and biomedical applications. Analytical Biochemistry, 2001, 298(1): 1–24
8. Zhang J, Fu Y, Lakowicz J R. Emission behavior of fluorescently labeled silver nanoshell: enhanced self-quenching by netal nanostructure. Journal of Physical Chemistry C, 2007, 111(5): 1955–1961
9. Lakowicz J R. Radiative decay engineering 5: metal-enhanced fluorescence and plasmon emission. Analytical Biochemistry, 2005, 337(2): 171–194
10. Bjerneld E J, Földes-Papp Z, Käll M, Rigler R. Single-molecule surface-enhanced raman and fluorescence correlation spectroscopy of horseradish peroxidase. Journal of Physical Chemistry B, 2002, 106(6): 1213–1218
11. Aslan K, Lakowicz J R, Geddes C D. Rapid deposition of triangular silver nanoplates on planar surfaces: application to metal-enhanced fluorescence. The Journal of Physical Chemistry B, 2005, 109(13): 6247–6251
12. Zhang Y X, Aslan K, Previte M J R, Geddes C D. Metal-enhanced fluorescence from copper substrates. Applied Physics Letters, 2007, 90(17): 173116
13. Baluschev S, Yu F, Miteva T, Ahl S, Yasuda A, Nelles G, Knoll W, Wegner G. Metal-enhanced up-conversion fluorescence: effective triplet-triplet annihilation near silver surface. Nano Letters, 2005, 5 (12): 2482–2484
14. Zhuo S J, Shao M W, Cheng L, Que R H, Zhuo S J, Ma D D D, Lee S T. Surface-enhanced fluorescence of praseodymium ions (Pr^{3+}) on silver/silicon nanostructure. Applied Physics Letters, 2010, 96 (10): 103108-1–103108-3
15. Ahrens B, Eisenschmidt C, Johnson J A, Miclea P T, Schweizer S. Structural and optical investigations of Nd-doped fluorozirconate-based glass ceramics for enhanced upconverted fluorescence. Applied Physics Letters, 2008, 92(6): 061905
16. Aisaka T, Fujii M, Hayashi S. Enhancement of upconversion luminescence of Er doped Al_2O_3 films by Ag island films. Applied Physics Letters, 2008, 92(13): 132105
17. Capobianco J A, Boyer J C, Vetrone F, Speghini A, Bettinelli M. Optical spectroscopy and upconversion studies of Ho^{3+}-doped Bulk and Nanocrystalline Y_2O_3. Chemistry of Materials, 2002, 14(7): 2915–2921
18. Bünzli J C G. Benefiting from the unique properties of lanthanide ions. Accounts of Chemical Research, 2006, 39(1): 53–61
19. Tissue B M. Synthesis and luminescence of lanthanide ions in nanoscale insulating hosts. Chemistry of Materials, 1998, 10(10): 2837–2845
20. Hasegawa Y, Wada Y, Yanagida S. Strategies for the design of luminescent lanthanide(III) complexes and their photonic applications. Journal of Photochemistry and Photobiology C, Photochemistry Reviews, 2004, 5(3): 183–202

21. Zhang J, Malicka J, Gryczynski I, Lakowicz J R. Surface-enhanced fluorescence of fluorescein-labeled oligonucleotides capped on silver nanoparticles. Journal of Physical Chemistry B, 2005, 109 (16): 7643–7648
22. Shao M W, Shan Y Y, Wong N B, Lee S T. Silicon nanowire sensors for bioanalytical application: glucose and hydrogen peroxide detection. Advanced Functional Materials, 2005, 15(9): 1478–1482
23. Lisiecki I, Pileni M P. Synthesis of copper metallic clusters using reverse micelles as microreactors. Journal of the American Chemical Society, 1993, 115(10): 3887–3896
24. Shao M W, Cheng L, Zhang X H, Ma D D D, Lee S T. Excellent photocatalysis of HF-treated silicon nanowires. Journal of the American Chemical Society, 2009, 131(49): 17738–17739
25. Tsang C H A, Liu Y, Kang Z H, Ma D D D, Wong N B, Lee S T. Metal (Cu, Au)-modified silicon nanowires for high-selectivity solvent-free hydrocarbon oxidation in air. Chemical Communications, 2009, (39): 5829–5831
26. Gunnarsson L, Bjerneld E J, Xu H, Petronis S, Kasemo B, Käll M. Interparticle coupling effects in nanofabricated substrates for surface-enhanced Raman scattering. Applied Physics Letters, 2001, 78(6): 802–804